

# Estimation of Specific Absorption Rate Using Infrared Thermography for the Biocompatibility of Wearable Wireless Devices

Varshini Karthik<sup>1</sup> and T. Rama Rao<sup>2, \*</sup>

**Abstract**—Wearable wireless technology has developed as an exciting topic over the last couple of years. With the extensive use of Wearable Wireless Devices (WWD) in greater proximity to the body for various wireless applications, the concern about biological effects due to the interaction of human tissues with the radiations is growing. In this research, we investigate the application of Infrared Thermography (IRT) to obtain temperature dynamics and reconstruct Specific Absorption Rate (SAR) to evaluate the exposure amenability of WWDs. A microstrip monopole antenna on a wearable substrate is used to determine the biological effects of the interaction of electromagnetic (EM) waves on the body. SAR is obtained using EM field simulations and by reconstruction from thermal measurements with the use of bio-heat equations for a continuous exposure of 300 s. Validation of IRT to reconstruct SAR is demonstrated by comparison with EM computations. The maximum SAR was 32 mW/kg, for simulations and 35 mW/kg, from reconstruction after IRT experiments. The maximum temperature change in both cases was always less than 1°C. The difference between the SAR obtained through IRT and simulation tools accounted for an average of 8.7%. Information acquired using IR temperature dynamics can yield SAR values which can assess radio frequency exposure compliance for WWD at frequencies used for modern wireless technologies, with reliability.

## 1. INTRODUCTION

Recently, there has been an exploding market for Wearable Wireless Devices (WWD) which by way of body-centric wireless communications (BCWC) aim at providing systems with constant availability, re-configurability, and unobtrusiveness [1]. Such a wearable scenario demands an emphasis on thermal, and biological aspects when Radio Frequency (RF) waves interact with the body. RF Waves have the ability to penetrate human tissues, cause oscillating electric fields, and human tissues absorb these fields and cause dielectric heating that manifests itself as temperature rise. The time rate at which RF energy is imparted to a mass of a biological tissue is Specific Absorption Rate (SAR). SAR values are dependent on morphological and electrical properties of tissues, antenna design, output power, distance from the body, placement and the transmitting device [2].

To ensure exposure compliance with Federal Communications Commission (FCC) and other regulatory agencies, the biological effects namely SAR and thermal effects of the RF-emitting devices must be measured. Electromagnetic (EM) simulation tools are often used to portray the antenna and human body interaction for the safety assessment of the RF antennas used with wearable devices. This method faces difficulty in realizing the intricate structures of the body and matching realistic physical settings [3, 4]. The differences between simulated and real-time measurements lower the precision of RF exposure compliance [5]. Conventional SAR measurement systems use physical  $E$ -field probes [6] in a liquid filled phantom, depicting the electrical properties of body tissues. The intrusive nature of

---

Received 26 February 2017, Accepted 20 April 2017, Scheduled 27 April 2017

\* Corresponding author: Thippiraju Rama Rao (ramaraotr@gmail.com).

<sup>1</sup> Department of Biomedical Engineering, SRM University, Chennai 603203, India. <sup>2</sup> RAMS Lab, Department of Telecommunication Engineering, SRM University, India.

the methodology, minutes of time consumed and the calibration requirements of the probe make the method cumbersome. It is thus seen that mathematical models, computer simulations, and phantom models are by so far the only available prospects for estimating SAR with considerable variation across them.

In addition to the use of SAR and power density measurements, temperature-based dosimetry systems are in vogue. Safe use of the antenna on the body is more related to temperature changes than power density [7]. Authors [8] in a review paper discussed that thermal effect is the only adverse effect of RF fields on aspects of human health. Researchers [9] have worked on bio thermal simulations to understand SAR and thermal distributions of UWB antennas on the human body while in [10] similar work for implanted UWB antenna was done. Numerical and experimental investigations on SAR and power density from heating dynamics on an experimental phantom was done by [11].

Recently, the authors in [12] have concluded that power density is not suitable to detect exposure compliance with millimeter wave devices when used close to the human body. They have proposed a temperature based technique using MRI for evaluation of safety compliance. MRI temperature mapping and understanding of RF heating while using MRI scanners for MRI compatible devices was given by [13, 14]. MRI temperature mapping to characterize heating from wireless devices that are not necessarily MRI compatible and calculation of 10 g average SAR using the heat mappings has been suggested by [15]. Accurate calculation of SAR using magnetic resonance temperature images and measured thermal properties of the phantom have been done by [16]. However, investigations on the EM exposure compliance through the use of Infrared Thermography, as a parallel technique to SAR and PD measurements, covering a broad range of present and future wireless technology bands have not been rigorously researched but has been proposed by [17].

The present study is designed to offer a solution for investigating the biological effects of modern day's wearable antennas from a thermal perspective using Infra-red thermography (IRT). First, numerical modeling is used to analyze SAR induced in a phantom, using RF/microwave exposure with recommended power levels for the various frequencies used. Second, IRT is used to investigate the direct manifestation of the EM waves' interaction with the body in terms of thermal changes during various intervals of exposure. Finally, SAR is reconstructed using the thermal dynamic measurements and one dimensional Bio-heat transfer equations. A comparative analysis between simulated and reconstructed values (using IRT) of SAR is done to understand the effectiveness of using IRT as an alternative technique for investigation of exposure compliance and reconstruction of SAR values.

## 2. PHANTOM MODEL OF HUMAN TISSUE AND ANTENNA DESIGN

### 2.1. Modelling Human Tissues for Simulations

A layered phantom model of human tissue, representing the outermost layers of the body namely skin, fat, muscle is considered. A layered model is chosen for its computational simplicity and accuracy. The interaction of the EM radiations with the tissues of the body at the cellular and molecular level [18] determine their electrical properties which vary with frequency. The electrical properties of the tissues at the various resonant frequencies of the designed antenna are based on the works of Italian National Research Council, which is available online [19] and are tabulated in Table 1. The design of wearable antenna deserves a complete understanding of the interaction and the electrical properties of body tissues. The tissue's water content affects the wavelength inside tissues [20]. Tissues having the highest water content have the highest relative permittivity (e.g., skin and muscle). The designed antenna is placed over the assembled tissues with an average thickness of 2 mm, 3.5 mm, 10 mm for skin, fat, muscle layer respectively as shown in Fig. 1.

### 2.2. Microstrip Antenna Design

The antenna design necessities for BCWCs differ from that of a conventional antenna designed for free space because of the tissue environment. An appropriate design of wearable antennas will guarantee minimum influence of the body on the antenna's performance and reduced emissions towards the body. Fig. 2 shows the dimensions and picture of the prototype of the wearable microstrip antenna. Microstrip model design equation [21] has been used for the design. The antenna is  $35 \times 32 \times 1.57 \text{ mm}^3$  in dimension

**Table 1.** Electrical properties of tissues at the four frequencies.

| Frequency (GHz) | Tissue | $\epsilon_r$ | $\sigma$ (S/m) | Tan $\theta$ (Loss tangent) |
|-----------------|--------|--------------|----------------|-----------------------------|
| 1.8             | Skin   | 38.8         | 1.18           | 0.30                        |
|                 | Fat    | 5.30         | 0.07           | 0.14                        |
|                 | Muscle | 53.5         | 1.34           | 0.25                        |
| 2.4             | Skin   | 38.0         | 1.44           | 0.28                        |
|                 | Fat    | 5.28         | 0.10           | 0.14                        |
|                 | Muscle | 52.7         | 1.70           | 0.24                        |
| 5.0             | Skin   | 35.7         | 3.06           | 0.30                        |
|                 | Fat    | 5.02         | 0.24           | 0.17                        |
|                 | Muscle | 49.5         | 4.04           | 0.29                        |
| 8.9             | Skin   | 32.3         | 6.78           | 0.42                        |
|                 | Fat    | 4.68         | 0.50           | 0.21                        |
|                 | Muscle | 44.2         | 9.05           | 0.41                        |

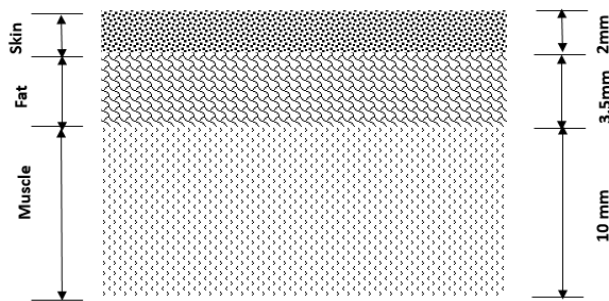


**Figure 1.** Layered model of human tissue.

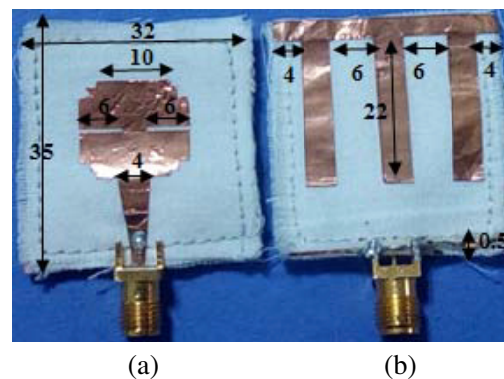


**Figure 2.** Photograph of the prototype of wearable microstrip antenna with the dimensions in mm for (a) radiating patch and (b) ground plane.

and is made of fabric cotton substrate that has a relative permittivity of 1.6 and loss tangent of  $4 \times 10^{-2}$ . The antenna is fabricated on the cotton substrate using a decal process. The antenna with a defected ground plane and a rectangular staircase patch is used for an optimized design. A step size of 1 mm followed by 1.5 mm from both top and bottom edges are used for the staircase arrangement. The radiating patch is fed by a  $50 \Omega$  microstrip line with a 1 mW power input at the port. A tapered microstrip line is used for good impedance matching. Design optimization is carried out to make the antenna perform at 1.8 GHz, 2.4 GHz, 5.0 GHz and 8.9 GHz with return loss less than  $-10$  dB as in Fig. 3. A partial ground plane is used to attain the multiband operation of the antenna. The shifted bands are aligned to the required resonant frequencies by utilizing the slots on the patch, and the staircase arrangement offers a greater value of return loss at different frequencies. EM compatibility with existing wireless technologies and unlicensed UWB is ensured by the choice of a multi-band operation.

### 3. SAR ASSESSMENT USING EM TOOLS

SAR is a good dosimetric quantity that measures the absorption of transmitted RF energy by human tissue. SAR is a function of the electrical conductivity, the induced  $E$ -field from the radiated energy, and the mass density of the tissue. SAR is calculated by averaging over a specific volume of the tissue,

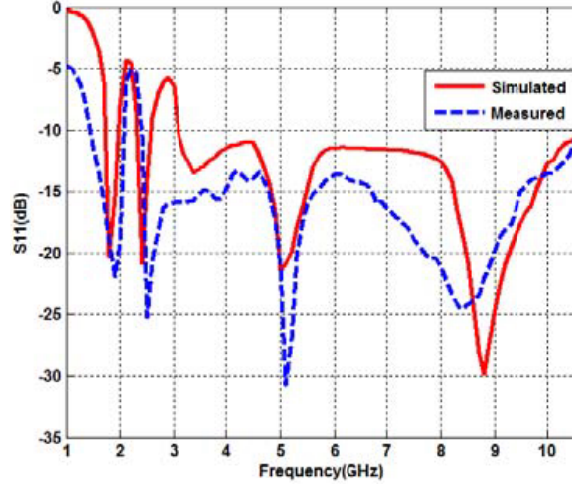


**Figure 3.** Simulated and measured return loss plot for on body placement of the antenna.

typically 1 gram or 10 grams. SAR is calculated as:

$$\text{SAR} = \frac{\sigma \cdot |E|^2}{\rho_m} \quad (1)$$

Here,  $E$  is the RMS value of the induced field in (V/m),  $\sigma$  the conductivity of tissue in (S/m), and  $\rho_m$  the mass density of tissue in  $\text{kg/m}^3$ .

EM field simulations were executed on the phantom-microstrip antenna arrangement. The Ansys HFSS simulation suite that uses finite time differentiation technique has been used. The SAR distribution and the average SAR values on the surface of the phantom (skin) in contact with the antenna are thus obtained. The net input power used was 1 mW. The body tissues that were incorporated into both EM field and SAR simulations had the properties as listed in Table 2. The SAR values were found to be far less than the maximum allowable limit of 2 W/kg averaged over 10 g of tissue exposed to EM radiations given by [22] and 1 g averaged SAR value of 1.6 W/kg given by [23] and are tabulated in Table 3.

**Table 2.** Parameter values of body tissues.

| Tissue/Parameter | Mass density<br>( $\text{kg/m}^3$ ) | Thermal conductivity<br>(W/m/K) | Heat capacity<br>(J/kg/K) |
|------------------|-------------------------------------|---------------------------------|---------------------------|
| Skin             | 1109                                | 0.37                            | 3391                      |
| Fat              | 911                                 | 0.21                            | 2348                      |
| Muscle           | 1090                                | 0.49                            | 3421                      |

**Table 3.** SAR values at four resonating frequencies on the forearm tissues.

| Frequency (GHz) | SAR (mW/kg) |     |        |
|-----------------|-------------|-----|--------|
|                 | Skin        | Fat | Muscle |
| 1.8             | 32          | 4.8 | 22     |
| 2.4             | 28          | 4.6 | 20     |
| 5.0             | 18          | 1.1 | 8.1    |
| 8.9             | 7.8         | 0.9 | 1.1    |

#### 4. SAR ASSESSMENT USING IR THERMOGRAPHY

##### 4.1. Experimental Setup for Temperature Dynamics Measurement

The IRT is an imaging modality using which the variations in temperature can be measured. An experimental setup to measure the thermal dynamics on the skin when exposed to the RF frequencies from the designed antenna is shown in Fig. 4. Measurements were made with healthy subjects with the region of interest at a distance of 1 m from the IR camera. A dark non-reflecting background was ensured to obtain thermograms using FLIR A305SC series IR camera. Thermograms thus obtained were analyzed using FLIR R&D research IR software tool.

The images were captured and analyzed under normal body condition of the subject. To ensure precision, the measurements were repeated three times with maintained environmental factors like room temperature and easing of the subjects in the set up room for 10 minutes before experiments. Thermograms were taken on the forearm, for the marked area of interest, revealing the skin temperature before placing the antenna and exciting it. The antenna was excited at 1.8, 2.4 and 5 GHz at 1.0 mW

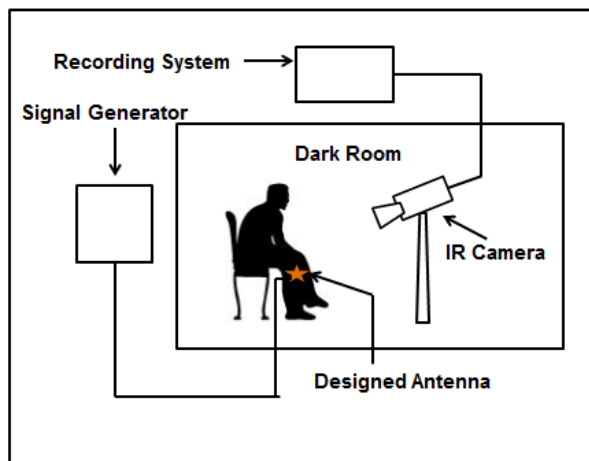


**Figure 4.** Experimental set up to obtain thermograms.

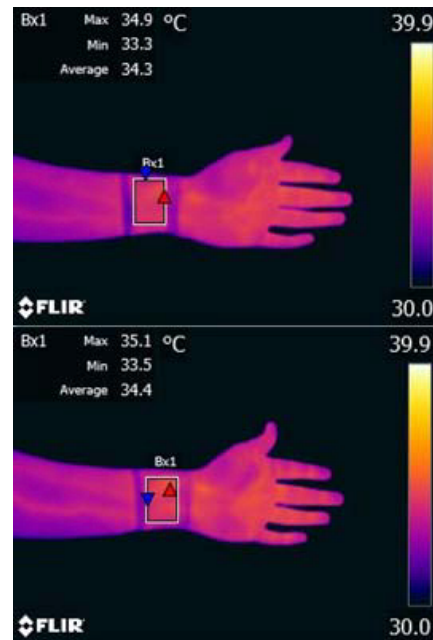


**Figure 5.** Sample thermogram at 0 and 10 minutes of emission from the wearable antenna on the forearm at 2.4 GHz.

**Table 4.** Temperature values from thermograms.

| Time (S) | Thermal values in °C using IR thermography |         |         |
|----------|--------------------------------------------|---------|---------|
|          | 1.8 GHz                                    | 2.4 GHz | 5.0 GHz |
| 0        | 0.00                                       | 0.00    | 0.00    |
| 60       | 0.15                                       | 0.10    | 0.05    |
| 120      | 0.20                                       | 0.15    | 0.10    |
| 180      | 0.25                                       | 0.25    | 0.15    |
| 240      | 0.30                                       | 0.30    | 0.25    |
| 300      | 0.35                                       | 0.35    | 0.30    |

power level by using Agilent’s N5182A MXG vector signal generator. Thermograms were taken for increasing time lapse of 60s, whose temperature values for a single subject are given in Table 4 and sample thermogram is shown in Fig. 5.

**4.2. Reconstruction of SAR Using Thermal Values**

The assessment of SAR from temperature data obtained from thermal images during the exposure of the human body to radio waves at 1.8, 2.4, and 5 GHz is done using the methodology shown in Fig. 6. The exposure is at GHz frequencies which has reduced penetration into the body tissues and hence very negligible increase in temperature noticed for very short term exposure in the order of a few seconds. A time duration of 300 s is chosen for thermography measurements and is for continuous radiation. It was observed that the temperature changes obtained through linear Equation (2) and by using Pennes’ Bio heat equation [24] for skin tissue through time evolution of temperature plot [25] gives almost same values for approximately 300 s of exposure. Beyond this time, thermoregulatory effects of conduction

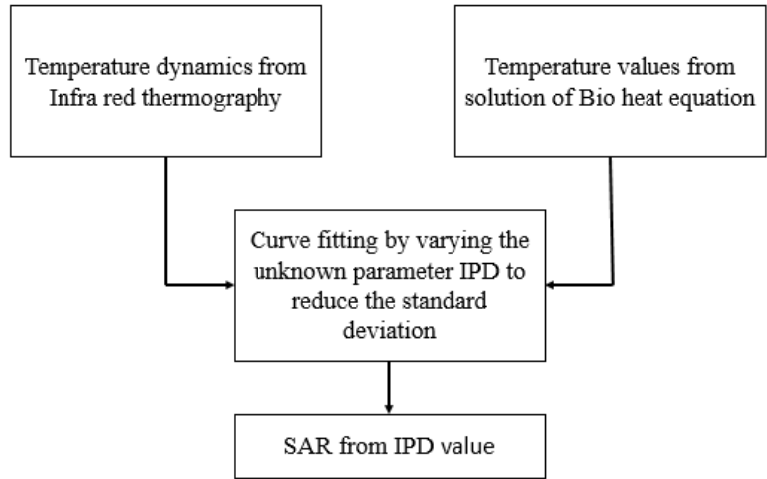


**Figure 6.** Reconstruction of SAR using IR thermography.

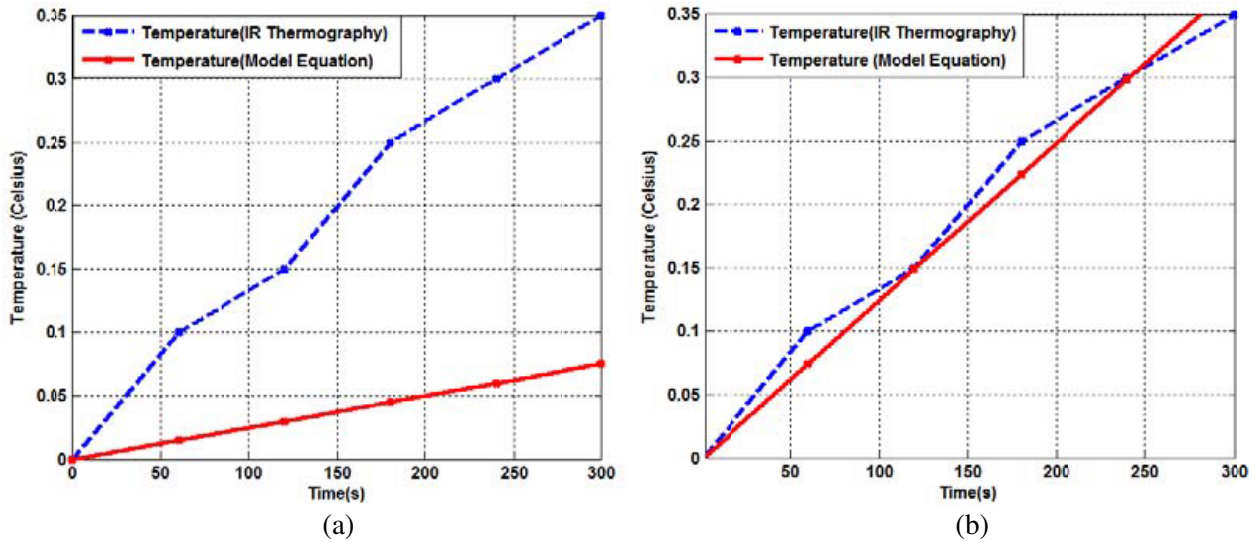


**Figure 7.** Temperature dynamics on skin at 2.4 GHz before (a) and after curve fitting (b) by varying the IPD.

and convection due to blood flow leads to an increase and then saturation of the graph. Hence the linear Equation (2) has been equated to Equation (3) [11] in the concept of estimation of SAR from thermography data for 300 s of continuous exposure. In the model equation for getting the temperature dynamics, obtained by equating (2) and (3),  $c$  is heat capacity of the tissue in J/kg/K,  $T$  is temperature in °C,  $t$  is time in seconds,  $r$  is power reflection coefficient calculated using VSWR of the antenna,  $d$  is penetration depth in  $m$  and  $p$  is tissue density in kg/m<sup>3</sup>. Using this model equation, theoretical values for change in temperature are found and are plotted. Initially incident power density (IPD) of 0.002 mW/cm<sup>2</sup> corresponding to input power of 1 mW is used in the model equation. The optimal value of IPD is then obtained through curve fitting shown in Fig. 7. Curve fitting is done to reduce the standard deviation between the theoretical and experimental thermodynamic plots and IPD that gives the best fitting curve is obtained. This optimal value of IPD is used to calculate the SAR using (3) and the same is tabulated in Table 5.

$$\text{SAR} = c \frac{\Delta T}{\Delta t} \quad (2)$$

$$c \frac{\Delta T}{\Delta t} = \text{SAR} = \frac{2 \cdot \text{IPD} \cdot (1 - r)}{d \cdot p} \quad (3)$$

#### 4.3. Comparative Analysis of Reconstructed and Simulated SAR Values

A comparison between the SAR values obtained from simulation tools on exciting the designed fabric antenna on human tissues and the values obtained from the thermal dynamics is made. The reconstructed value of SAR using the IR thermography technique and the Bio heat model equations are analyzed for its difference with the simulated values. An average difference in SAR using the two methods is found to be 8.7% as shown in Table 5. This shows a good agreement between both the methods.

**Table 5.** Comparitvie analysis of reconstructed and simulated SAR values.

| Operating frequency (GHz)                       | SAR (mW/kg)            |                     | Difference in SAR using the two methods |
|-------------------------------------------------|------------------------|---------------------|-----------------------------------------|
|                                                 | Thermography technique | Simulation software |                                         |
| 1.8                                             | 35                     | 32                  | 8.9%                                    |
| 2.4                                             | 30                     | 28                  | 6.8%                                    |
| 5.0                                             | 20                     | 18                  | 10.5%                                   |
| Average difference in SAR using the two methods |                        |                     | 8.7%                                    |

## 5. DISCUSSIONS AND CONCLUSIONS

An infrared temperature based technique for wearable wireless device exposure compliance evaluation with a microstrip monopole antenna has been presented in this research. The results of this study exhibit the use of IRT for safety evaluation of RF/microwave emissions from wearable devices, using the ability to detect temperature changes on the surface of the body. Furthermore, this study illustrates that IR temperature-based RF safety evaluation can be used in a generic way for compliance assessments of wearable wireless devices working at different frequencies and power levels. Reconstruction of SAR from temperature dynamics and model bio-heat equation for 300 s of exposure was introduced and computed. Orientation of simulated and experimental temperature dynamics and SAR are serious and significant care was taken to imitate the electrical and physical attributes of the body tissues. The maximum SAR was 32 mW/kg, for simulations and 35 mW/kg, from reconstruction subsequent to IRT experiments using the maximum output power as 1 mW. This resulted in SAR values that are very much compliant with the international safety limits of 2 W/kg. The maximum temperature elevation in both cases was always less than 1°C. The difference between the SAR values obtained through IRT and simulation tools accounted to an average of 8.7%. The capability to quantify 32 mW/kg of power deposited is not

a lower bound for the sensitivity of the measurement. Since the method is based on IR temperature measurements, improvement in the accuracy and sensitivity of the IR thermometry tools will permit computation of smaller SAR values. Evaluation of SAR using IRT for high frequency microwave devices, would require longer heating periods, as the penetration depth is smaller. SAR determination using the proposed method can be probed for various upper and lower bounds of the dynamic range given in terms of temperature increase, heating time and power levels.

## ACKNOWLEDGMENT

Authors are highly appreciative to the DRDO, Govt. of India for their support in executing this research.

## REFERENCES

1. Hall, P. S. and Y. Hao, *Antennas and Propagation for Body-centric Wireless Communications*, 2nd Edition, Artech House, 2012.
2. Christ, A., M. C. Gosselin, M. Christopoulou, S. Kuhn, and N. Kuster, "Age-dependent tissue-specific exposure of cell phone users," *Phys. Med. Biol.*, Vol. 55, 1767–1783, 2010.
3. Brishoual, M., C. Dale, J. Wiart, and J. Citerne, "Methodology to interpolate and extrapolate SAR measurements in a volume in dosimetric experiment," *IEEE Trans. Electromagn. Compat.*, Vol. 43, 382–389, 2001.
4. Chavannes, N., R. Tay, N. Nikoloski, and N. Kuster, "Suitability of FDTD-based TCAD tools for RF design of mobile phones," *IEEE Antennas and Propagation Magazine*, Vol. 45, 52–66, 2003.
5. Schmid, T., O. Egger, and N. Kuster, "Automated *E*-field scanning system for dosimetric assessments," *IEEE Transactions on Microwave Theory and Techniques*, Vol. 44, 105–113, 1996.
6. Institute of Electrical and Electronics Engineers Recommended practice for determining the peak spatial-average SAR in the human head from wireless communications devices: Measurement techniques, IEEE Standard 1528-2013, 2013.
7. Wu, T., T. S. Rappaport, and C. M. Collins, "The human body and millimeter-wave wireless communication systems: Interactions and implications," *2015 IEEE International Conference on Communications (ICC)*, 2423–2429, IEEE, 2015.
8. Chou, C. K. and J. A. D'Andrea, "Reviews of effects of RF fields on various aspects of human health: Introduction," *Bioelectromagnetics*, Vol. 24.S6, 2003.
9. Tuovinen, T., M. Berg, K. Y. Yazdandoost, and J. Linatti, "On the evaluation of biological effects of wearable antennas on contact with dispersive medium in terms of SAR and bio-heat by using FIT technique," *ISMICT*, 149–153, Tokyo, Mar. 2013.
10. Thotahewa, K. M., J. M. Redouté, and M. R. Yuce, "SAR, SA, and temperature variation in the human head caused by IR-UWB implants operating at 4 GHz," *IEEE Transactions on Microwave Theory and Techniques*, Vol. 61, No. 5, 2161–2169, 2013.
11. Zhadobov, M., N. Chahat, R. Sauleau, C. Le Queument, and Y. Le Drean, "Millimeter-wave interactions with the human body: State of knowledge and recent advances," *International Journal of Microwave and Wireless Technologies*, Vol. 3, No. 2, 237–247, 2011.
12. Wu, T., T. S. Rappaport, and C. M. Collin, "Safe for generations to come: Considerations of safety for millimeter waves in wireless communications," *IEEE Microwave Magazine*, Vol. 16, No. 2, 65–84, 2015.
13. Sankaralingam, S. and B. Gupta, "Development of textile antennas for body wearable applications and investigations on their performance under bent conditions," *Progress In Electromagnetics Research B*, Vol. 22, 53–71, 2010.
14. Florence, E. S., M. Kanagasabai, and G. N. M. Alsath, "An investigation of a wearable antenna using human body modelling," *Applied Computational Electromagnetics Society Journal*, Vol. 29, No. 10, 2014.



15. Alon, L., G. Y. Cho, X. Yang, D. K. Sodickson, and C. M. Deniz, "A method for safety testing of radiofrequency/microwave-emitting devices using MRI," *Magnetic Resonance in Medicine*, Vol. 74, No. 5, 1397–1405, 2015.
16. Alon, L., D. K. Sodickson, and C. M. Deniz, "Heat equation inversion framework for average SAR calculation from magnetic resonance thermal imaging," *Bioelectromagnetics*, Vol. 37, No. 7, 493–503, 2016.
17. Karthik, V. and T. Rama Rao, "Thermal distribution based investigations on electromagnetic interactions with the human body for wearable wireless devices," *Progress In Electromagnetics Research M*, Vol. 50, 141–150, 2016.
18. Gabriel, C., S. Gabriely, and E. Corthout, "The dielectric properties of biological tissues: I. Literature survey," *Phys. Med. Biol.*, Vol. 41, 2231–2249, 1996.
19. Italian National Research Council, Institute for Applied Physics, homepage on Dielectric properties of body tissues. [Online]. Available: <http://niremf.ifac.cnr.it>.
20. Tuovinen, T., M. Berg, K. Y. Yazdandoost, and J. Linatti, "Ultra wideband loop antenna on contact with human body tissues," *IET Microwave and Antennas Propagation*, Vol. 7, No. 7, 588–596, 2013.
21. Garg, R., P. Bhartia, I. Bahl, and A. Ittipiboon, *Microstrip Antenna Design Handbook*, Artech House, 2001.
22. Allen, S. G., et al., "ICNIRP guidelines for limiting to time varying electric, magnetic, and electromagnetic fields (upto 300 GHz)," *Health Physics*, Vol. 74, No. 4, 494–522, 1998.
23. IEEE Standard for Safety Levels with Respect to Human Exposure to the Radio Frequency Electromagnetic Fields 3 kHz to 300 GHz, IEEE Std. C95.1, 2005.
24. Kritikos, H. N., P. Herman, and Schwan, "Potential temperature rise induced by electromagnetic-field in brain tissues," *IEEE Trans. on Biomedical Engineering*, Vol. 26, No. 1, 29–34, 1979.
25. Karthik, V. and T. Rama Rao, "Investigations on SAR and thermal effects of a body wearable microstrip antenna," *Wireless Personal Communications*, 1–17, 2017, DOI: 10.1007/s11277-017-4059-9.